Impact of DFIG in Wind Energy Conversion System for Grid Disturbances

Sasmita Behera[*], Sudeep Kumar Behera, Bibhuti Bhusan Pati

Department of Electrical & Electronics Engineering, Veer Surendra Sai University of Technology, Burla, Odisha, India

Abstract

In this work, a grid-connected DoublyFed Induction Generator (DFIG) is studied for the transient and steady response. The vector control technique controls the Pulse Width Modulation (PWM) of both the back-to-back converters interfacing rotor to the grid. Reactive power supply and DC bus voltage are managed by the grid-side inverter. Active power and rotor angular speed are adjusted by the machine side inverter facilitating power generation for varying wind. The effect of voltage and frequency deviation from the grid on the control is observed. The controllers are found to work satisfactorily except for large frequency variation. The current harmonics are also within the allowed limit. The proposed controllers are expected to satisfy the revised grid code for wind energy.

Keywords: vector control, PWM, voltage sag, voltage swells

1. Introduction

Increasing share of wind power in grid connection draws attention to the study of its effect on power system stability. In the Wind Energy Conversion System (WECS), different generators are in use. The majority of variable speed WECS have Doubly Fed Induction Generator (DFIG) [1]. This is due to the efficient energy conversion, low cost, less mechanical stress etc. [2]. The increased proportion of wind power has forced the grid codes to be modified from its isolation by crowbar [1] to ride through the control during the grid disturbance [3]. Active and reactive power control for changing wind speed is accomplished by a stator flux oriented vector control with its real axis aligned to the stator flux vector rotating at the synchronous speed in [4]. The performance of such a system for various balanced and unbalanced fault conditions is explored in [5-6]. There are many possible ways to control the outputs of the generator with different orientation of the real axis of the reference frame [7]. Minor but frequent disturbances in the grid such as voltage dip, sag and swell in the grid lead to poor of power quality, reliability,and equipment failure [8]. Such disturbances associated with voltage can be supplemented by reactive power balance. Different external reactive power support devices have also been in research, but with the additional cost [9-11]. In [12], upholding of DFIG by internal control for low voltage in stator voltage oriented reference frame is studied. In another study, the swell case of voltage is observed in [13]. Xiao et al. [14] have tentatively defined a maximum limit beyond which the crowbar protection should be activated. Selectively harmonics have been eliminated by proper control of DFIG in [15]. To minimize rotor current that activates crowbar during low voltage, additional feed-forward control has been proposed in [16]. Instead of voltage oriented vector control, a direct current control [17] has been proposed for faster control. Mohseni et al. [18-20] have proposed switching to hysteresis control during transient rather than utilizing Proportional-Integral (PI) current control for steady-state in order to satisfy grid code for the ride-through requirement. But, harmonics with hysteresis control is beyond the standard. PI with resonance control has been proposed in [21-22], to reduce torque pulsation and unbalanced voltage [23]. In addition, to reduce the transient time, torque oscillation for voltage swells virtual impedance control strategy has been proposed in [24].

*Corresponding author. E-mail address:sasmitabehera2000m@gmail.com

The Model Predictive Control (MPC) for switching converter instead of PWM has been reviewed in [25]. Though it was faster than PWM, the THD and steady-state performance were inferior. In a comparative study, Tremblay et al. [26] have shown robustness to noise and better control of the DFIG by PI control in vector control in comparison to Direct Power Control (DPC) and Direct Torque Control (DTC) approach. In recent literature, a demagnetizing current control based on vector control has been proposed for faster control for low voltage [27]. The studies are also limited to sag, swell or harmonic reduction. Having reviewed the literature for improvement of control to meet the latest grid codes for WECS, the vector control with PI controller is still unsurpassed though many other control techniques, which have been developed [28-32]. Herein, the vector control technique controls the PWM of both the back to back converters interfacing rotor to the grid to maintain reliable power. The sections 2-5 embody the equations governing the different parts of the model. Response to grid disturbances is presented in section 6 concluding the impact of DFIG in this condition.

2. Model of WT-DFIG System

The power of the wind drives the Wind Turbine (WT) coupled to DFIG. With the gearbox in between, the rotational speed is stepped up suitably and the DFIG generates electricity from the mechanical input. Fig. 1 shows a DFIG vector control strategy. For the accurate design of the dynamic model in the d-q frame, the transient reactance of the generator is considered. The equivalent circuits of DFIG and induction machine are analogous [7, 33].
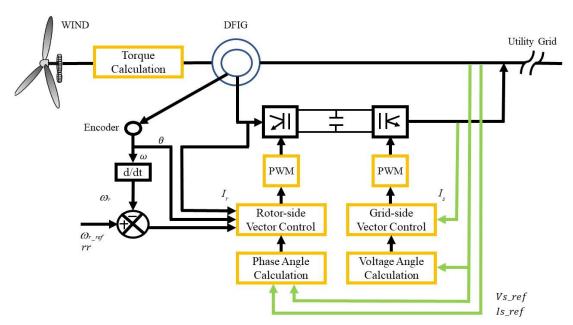

Fig. 1 Overall structure of the DFIG model

Definingthe different electrical circuit parameters in the d-q frame as in Eqs. (1-5), it yields

$$E_d^{'} = -(\frac{\omega_s L_{ss}}{L_{rr}})\psi_{qr} \tag{1}$$

$$E_q^{'} = -(\frac{\omega_s L_m}{L_{rr}})\psi_{dr} \tag{2}$$

$$X_s = \omega_s L_{ss} \tag{3}$$

$$X_s^{'} = \omega_s \left[L_{ss} - \left(\frac{L_m^2}{L_{rr}} \right) \right] \tag{4}$$

$$T_0^{'} = -\frac{L_{rr}}{R_r} \tag{5}$$

the DFIG is modelled as in Eqs. (6) to (10) :

$$\frac{X_s' di_{ds}}{\omega_s dt} = v_{ds} - \left[R_s + \frac{1}{\omega_s T_0'}\left(X_s - X_s'\right)\right]i_{ds} - (1-s)E_d' - \frac{L_m}{L_{rr}}v_{dr} + \frac{1}{\omega_s T_0'}E_q' + X_s' i_{qs} \tag{6}$$

$$\frac{X_s' di_{qs}}{\omega_s dt} = v_{qs} - \left[R_s + \frac{1}{\omega_s T_0'}\left(X_s - X_s'\right)\right]i_{qs} - (1-s)E_q' - \frac{L_m}{L_{rr}}v_{qr} - \frac{1}{\omega_s T_0'}E_q' - X_s' i_{ds} \tag{7}$$

$$\frac{dE_d'}{dt} = \omega_s E_q' - \omega_s \frac{L_m}{L_{rr}}v_{qr} - \frac{1}{T_0'}\left[E_d' + \left(X_s - X_s'\right)i_{qs}\right] \tag{8}$$

$$\frac{dE_q'}{dt} = \omega_s E_d' + \omega_s \frac{L_m}{L_{rr}}v_{dr} - \frac{1}{T_0'}\left[E_q' - \left(X_s - X_s'\right)i_{ds}\right] \tag{9}$$

$$\Psi_{dr} = L_{rr}i_{dr} + L_m i_{ds} \tag{10}$$

$$\Psi_{qr} = L_{rr}i_{qr} + L_m i_{qs} \tag{11}$$

where ψ , L , R , X , v , E , i are flux linkage, inductance, reactance, voltage, emf, and current respectively. The first subscript d, q stands for the directors and the quadrature component respectively, and the second subscript r and s represent as rotor and stator respectively. The repetition of subscript s and r for L stand for the corresponding self-inductance, whereas single m stands for mutual inductance. ω_t is the synchronous speed, s is the slip, T_0' is the electrical time constant of the rotor, the superscript $'$ represents a transient condition.

Equating the LHS of Eqs. (3) and (4), and neglecting rotor resistance v_{ds} .Then substituting for Ψ_{dr} and Ψ_{qr} , it reduces to

$$V_{dr} = -(\omega_s - \omega_r)L_{rr}i_{qr} - (\omega_s - \omega_r)L_m i_{qs} \tag{12}$$

$$V_{qr} = (\omega_s - \omega_r)L_{rr}i_{dr} + (\omega_s - \omega_r)L_m i_{ds} \tag{13}$$

3. The Drive Train

To model drive train, the two-mass model is simple and it amply represents the dynamics of WT suitable for transient state analysis [34]. The two masses are the generator-gearbox and the hub with blades. Mathematically, it is expressed by

$$2H_t \frac{d\omega_s}{dt} = T_w - T_s \tag{14}$$

$$\frac{d\theta_t}{dt} = \omega_t - \omega_r = \omega_t - (1-s)\omega_s \tag{15}$$

$$2H_g \frac{ds}{dt} = -T_e - T_s \tag{16}$$

$$T_s = K_s \theta_t + D_s \frac{d\theta_t}{dt} \tag{17}$$

where H_t and H_g represent the inertia of the hub and the generator, respectively, ω_t is the turbine angular speed, ω_r is the generator rotor angular speed, θ_t is the shaft torsion angle, D_s and K_s are the is the stiffness and damping coefficients of shaft respectively, T_s is the shaft torque, T_w is the effective torque input to the WT, T_e is the electromagnetic torque. T_w and T_e are given by

$$T_w = \frac{0.5 \rho_a \pi R^2 C_p}{\omega_t} V_w^3 \tag{18}$$

$$T_e = P_s / \omega_s \tag{19}$$

$$C_p = 0.5176(\frac{116}{\lambda_i} - 0.4\beta - 5)e^{-2\frac{1}{\lambda_i}} + 0.0068\lambda \tag{20}$$

$$\frac{1}{\lambda_i} = \frac{1}{\lambda + 0.08\beta} - \frac{0.035}{1 + \beta^3} \tag{21}$$

$$\lambda = \frac{\omega_t R}{V_w} \tag{22}$$

where P_a is the air density, R is the radius swept by WT blade, V_w is the velocity of wind, β is the pitch angle, λ is the blade tip speed ratio, P_s is the stator active power, C_p is the power coefficient. By controlling ω_t, maximum C_p and maximum power from wind can be achieved.

4. Converter Modeling

From Fig. 2(b), the active power equation is:

$$P_r = P_g + P_{DC} \tag{23}$$

where P_r is the rotor power that charges the DC bus capacitor with P_{DC}, and delivers P_g to the grid. These are given by

$$P_r = v_{dr}i_{dr} + v_{qr}i_{qr} \tag{24}$$

$$P_g = v_{dg}i_{dg} + v_{qg}i_{qg} \tag{25}$$

$$P_{DC} = v_{DC}i_{DC} = -Cv_{DC}\frac{dv_{DC}}{dt} \tag{26}$$

where v stands for the voltage and i the current with the second subscript r and g represent for rotor and grid respectively. v_{DC}, i_{DC} and C are the voltage, current, and capacitance of the capacitor in DC link.

Now, rewriting Eq. (18), the power balance in terms of voltages and currents gives:

$$C_{VDC}\frac{dv_{DC}}{dt} = v_{dg}i_{dg} + v_{qg}i_{qg} - (v_{dr}i_{dr} + v_{qr}i_{qr}) \tag{27}$$

5. Controller Modeling

Fixing d-axis of the $d - q$ reference frame with v_{ds}, v_{qs} nullifies and v_{ds} equals the grid voltage. P_g and reactive power Q_g can be regulated separately by i_{dg} and i_{qg} respectively in a decoupled manner by vector control resolving three phases to $d - q$ components [35]. The stator active power and voltage can also be adjusted separately by v_{qr} and v_{dr} as described below.

5.1.Machine-side control

The controller on the rotor-side retains the terminal voltage to set point and controls the DFIG output active power varying with the WT torque [27]. The control of active power and voltage are achieved by v_{qr} and v_{dr}, respectively. The control structure is given in Fig. 2(a), while the control is expressed as:

$$v_{qr} = K_{p2}\left(K_{p1}\,\Delta p + K_{i1}x_1 - i_{qr}\right) + K_{i2}x_2 + s_r\omega_s L_m i_{ds} + s_r\omega_s L_{rr} i_{qr} \tag{28}$$

$$v_{dr} = K_{p2}\left(K_{p3}\,\Delta v + K_{i3}x_3 - i_{dr}\right) + K_{i2}x_4 - s_r\omega_s L_{rr} i_{dr} \tag{29}$$

where the gain of the PI controller is K_{xy}. The first subscript x with notation p and i represent proportional and integral gains respectively. The second subscript 1, 2, 3 are for the power controller, machine-side current controller, and grid voltage controller, respectively. $i_{dg} - r_{ef}$ and $i_{dg} - r_{ef}$ are the references for the respectivecomponents of the current on the rotor, v_{s-ref} is the reference for stator terminal, P_{ref} is the reference of active powerfound from

$$P_{ref} = P_B \frac{\omega_t}{\omega_{tB}} \tag{30}$$

where ω_{tB} is the WT angular speed base, P_B is the maximum output active power at ω_{tB}.

5.2.Grid-side control

The grid-side converter controller (Fig. 2(b)), controls v_{DC} by i_{dg} and the reactive power by i_{dg}. The change in intermediary states x_1, x_2 and x_3, shown in Fig. 2(b) are expressed as:

$$\frac{dx_1}{dt} = v_{DC-ref} - v_{DC} = \Delta v_{DC} \tag{31}$$

$$\frac{dx_2}{dt} = i_{dg-ref} - i_{dg} = K_{pdg}\Delta v_{DC} + K_{Idg}x_1 - i_{dg} \tag{32}$$

$$\frac{dx_3}{dt} = i_{qg-ref} - i_{qg} \tag{33}$$

$$\Delta v_{dg} = K_{pg}\frac{dx_2}{dt} + K_{Ig}x_2 \tag{34}$$

$$\Delta v_{qg} = K_{pg}\frac{dx_3}{dt} + K_{Ig}x_3 \tag{35}$$

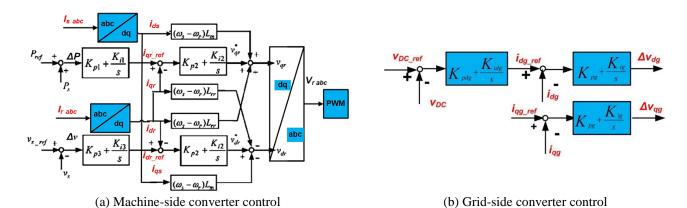(a) Machine-side converter control   (b) Grid-side converter control

Fig. 2 The control of converters [12]

where K_{pdg} and K_{Idg} are the proportional and integral gains of the DC bus voltage controller, respectively. Its output $i_{dg} - r_{ef}$ is the set point for i_{dg}; K_{pg} and K_{Ig} are the proportional and integral gains of the grid-side converter current regulator, respectively, $v_{DC} - r_{ef}$ is the DC bus voltage set point and $i_{dq} - r_{ef}$ is the reference for i_{dq} [7]. DC link voltage drop due to increased active power demand due to or wind speed variation in sub-synchronous speed operation is controlled by a change in Δv_{dg} (cf. Eq. (22)). Reactive power is controlled by controlling Δv_{dg}. PWM gating pulses are generated in a similar manner from above two grid voltages as shown in Fig. 2(a).

6. Result Discussion

The WECS considered is integrated to a 120 kV, 3 phase 2500 MVA grid with transformers in between. The model is built in MATLAB/SIMULINK with system specifications: V_w :15 m/s,DFIG: 9kW, 575 V, 6 pole, 1440 rpm, 60 Hz; DC bus voltage 1150 V with a capacitor of 60 mF; frequency of the PWM carriers 1.62 kHz and 2.7 kHz for machine-side and grid-side converters respectively.To reduce the injection of harmonics from DFIG via the grid side converter to the grid, the switching frequency is kept high.

6.1. Balanced grid

The stator currents and voltages of DFIG under steady-state condition (the wind speed constant at 15m/s) are depicted in Fig. 3(a). The active power (blue) produced by DFIG is 0.9 PU which is excluding electromechanical losses from the mechanical input, which is similar to the findings in [4]. The reactive power (green) reference is 0 kVAR. The DC bus voltage remains stable at 1150 V. The rotor angular speed is 1.2 PU, the rated value.
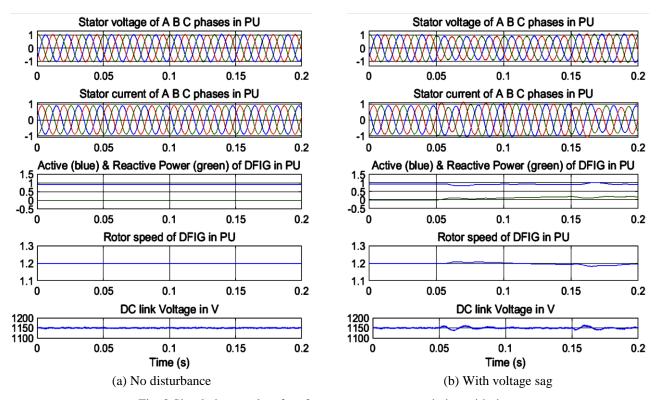

(a) No disturbance   (b) With voltage sag

Fig. 3 Simulation results of performance parameter variation with times

6.2. Voltage sag on the grid

Grid voltage sag occurs due to generation outage, line outage and switching of a heavy fluctuating load. When voltage sag of 0.15 PU [16, 21] is uniformly applied in all phases at 0.05 s for 9 cycles, the effects are depicted in Fig. 3(b). Normally the deviation is limited to ±10% as per IEEE 1159. Abnormal violations of grid voltage, which sag beyond ±10%, are taken to verify the effectiveness of the control system. On abrupt deviation of the grid voltage from its rated, the stator current rises and the active power P fluctuates and the active power control competently brings it to its rating within the next 4 cycles. For voltage sag reactive power is supported by DFIG with an increased injection of Δv_{qg} and adjusting Δv_{dr} . It supplies reactive power to the grid at that time and settles to 0 kVAR by appropriate control action. For a variation of up to 25%, such rise of current due to sag has a negligible effect on DFIG and the controller works well. The DC bus voltage oscillates at the switching instants and comes down to its set value of 1150 V by the grid side converter. The rotor speed is constant (1.2 PU) as V_w is fixed.

6.3. Voltage swells on the grid

Under symmetrical rise of voltage by 0.2 PU at 0.05 s continuing for 9 cycles, the variations are depicted in Fig. 4(a).The grid voltage may swell under outage of a large load. When the grid voltage swells, the stator current falls to maintain powerconstant. The reactive power Q falls suddenly due to a decrease in power demand and then comes back to 0 kVAR within 4 cycles which is better than that in [8] and [13]. It sustains as per Australian grid code [20]. Finally, the system settles to its set value.

6.4. Fall of grid frequency

When the grid frequency drops from 60 Hz rated to 58 Hz at 0.05 s, the proposed control strategy does not act upon it as seen from Fig. 4(b). Such condition of frequency fall may arise due to loss of large generation. Though the case is quite unusual, as the IEC standard limits grid frequency deviation to ±0.5 Hz, it is shown to check the prominent effect in the simulation. It is indicative of the modification of control required to counter to such large change in frequency. However, for the deviation within standard limits the controller performs to stabilize. Since the machine rated frequency is 60 Hz, it is not responding to 58 Hz, and the machine collapses with a gradual fall of rotor angular speed and DC bus voltage. Compared to the grid, the capacity of the generator is small, hence this DFIG can't support frequency stabilization of the grid.
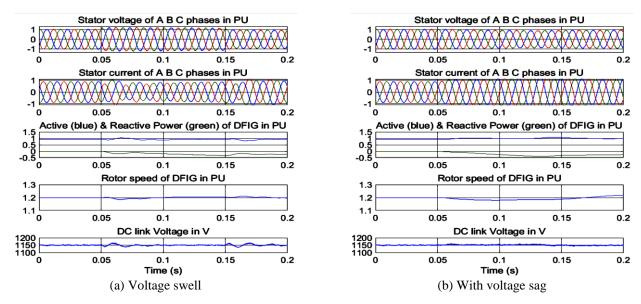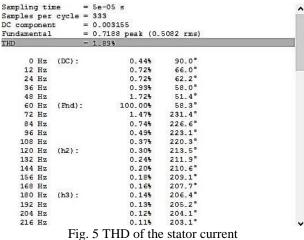

(a) Voltage swell   (b) With voltage sag

Fig. 4 Simulation results of performance parameters variation with times

6.5. Current harmonics

Fig. 5 THD of the stator current

The harmonics in the stator current of the DFIG are also analyzed and given in Fig. 5. The dominant odd harmonics have suppressed considerably. The THD is 1.89 %, which is satisfied as per the standards.

7. Conclusions

A DFIG-WT system with a back-to-back VSC is studied with its PWM controlled by PI controllers without a crowbar. The impact of DFIG is investigated under steady state, for a large deviation of ±20% in voltage and 3% in the frequency of the grid. The stator voltage, current, active and reactive power exchange between the grid and the DFIG are observed. In conclusion, the DFIG supports grid within stability limits for the cases being discussed except for variation in frequency with the implementation of the vector control strategy. In the grid-connected DFIG, the harmonic suppression measure has already been presented. Since the harmonicfilter at the input to the controller, it is expected that the control will work in the presence of harmonics. The stator current has 1.89% THD, well within the limit. Further study can be focused on the improvement of control performance in the larger rating of DFIG and unbalanced faults.

Acknowledgement

Conflicts of Interest

The authors declare no conflict of interest.

References

[1] J. López, E. Gubía, E. Olea, J. Ruiz, and L. Marroyo, "Ride through of wind turbines with doubly fed induction generator under symmetrical voltage dips,"IEEE Transactions on Industrial Electronics,vol. 56, no. 10, pp. 4246-4254, 2009.

[2] R. Mittal, K.S. Sandhu, and D.K. Jain, "An overview of some important issues related to wind energy conversion system (WECS)," International Journal of Environmental Science and Development, vol. 1, no. 4, pp. 351-363, 2010.

[3] A.K. Pathak, M.P. Sharma, and M. Bundele, "A critical review of voltage and reactive power management of wind farms,"Renewable and Sustainable Energy Reviews,vol. 51, pp. 460-471, 2015.

[4] B. C. Babu and K.B. Mohanty, "Doubly-fed induction generator for variable speed wind energy conversion systems-modeling &simulation," International Journal of Computer and Electrical Engineering, vol. 2, no. 1, pp. 1793-1806, February, 2010.

[5] K. S. Rao and M. V. Kumar, "Analysis of doubly fed induction generator under varies fault conditions," International Journal of Engineering Research and Applications, vol. 3, no. 6, pp. 2102-2106, November-December 2013.

[6] X. Yan, G. Venkataramanan, P.S. Flannery, Y. Wang, and B. Zhang, "Evaluation of the effect of voltage sags due to grid balanced and unbalanced faults on DFIG wind turbines,"European Power Electronics and Drives Journal,vol. 20, no. 4, pp. 51-61, 2010.

[7] F. Wu, X.P. Zhang, K. Godfrey, and P. Ju, "Small signal stability analysis and optimal control of a wind turbine with doubly fed induction generator,"IET Generation, Transmission and Distribution,vol. 1, no. 5, pp. 751-760, 2007.

[8] N. Edomah, "Effects of voltage sags, swell and other disturbances on electrical equipment and their economic implications," In IET Electricity Distribution-Part 1, 20th International Conference and Exhibition onCIRED, 2009, pp. 1-4.

[9] M.E. Hossain, "Low voltage ride-through capability improvement methods for DFIG based wind farm,"Journal of Electrical Systems and Information Technology, vol. 5, no. 3, 2018.

[10] S. Agalar and Y.A. Kaplan, "Power quality improvement using STS and DVR in wind energy system,"Renewable Energy,vol. 118, pp. 1031-1040, 2018.

[11] S. Priyavarthini, C. Nagamani, G.S. Ilango, and M.A. A. Rani, "An improved control for simultaneous sag/swell mitigation and reactive power support in a grid-connected wind farm with DVR,"International Journal of Electrical Power and Energy Systems,vol. 101, pp. 38-49, 2018.

[12] R. D. Shukla and R. K. Tripathi, "Dynamic performance of DFIG based WECS under different voltage sag,"International Journal of Chemtech Research,vol. 5, no. 2, pp. 980-992, 2013.

[13] S. Choudhury, K.B. Mohanty, and B.K. Debta, "Investigation on performance of Doubly-fed induction generator driven by wind turbine under grid voltage fluctuation," InIEEE 10thInternational Conference onEnvironment and Electrical Engineering, 2011, pp. 1-4.

[14] S. Xiao, H. Geng, H. Zhou, and G. Yang, "Analysis of the control limit for rotor-side converter of doubly fed induction generator-based wind energy conversion system under various voltage dips,"IET Renewable Power Generation,vol. 7 no. 1, pp. 71-81, 2013.

[15] M. Kesraoui, A. Chaib, A. Meziane, and A. Boulezaz, "Using a DFIG based wind turbine for grid current harmonics filtering,"Energy Conversion and Management,vol. 78, pp. 968-975, 2014.

[16] J. Liang, W. Qiao, and R.G. Harley, "Feed-forward transient current control for low-voltage ride-through enhancement of DFIG wind turbines,"IEEE Transactions on Energy Conversion,vol. 25, no. 3, pp. 836-843, 2010.

[17] S. Li, T.A. Haskew, K.A. Williams, and R.P. Swatloski, "Control of DFIG wind turbine with direct-current vector control configuration,"IEEE transactions on Sustainable Energy,vol. 3, no. 1, pp. 1-11, 2012.

[18] M. Mohseni, M.A. S. Masoum, and S.M. Islam, "Low and high voltage ride-through of DFIG wind turbines using hybrid current controlled converters,"Electric Power Systems Research,vol. 81, no. 7, pp. 1456-1465, 2011.

[19] M. Mohseni, S.M. Islam, and M. A. S. Masoum, "Enhanced hysteresis-based current regulators in vector control of DFIG wind turbines,"IEEE Transactions on Power Electronics,vol. 26, no. 1, pp. 223-234, 2011.

[20] M. Mohseni and S.M. Islam, "Transient control of DFIG-based wind power plants in compliance with the Australian grid code,"IEEE Transactions on Power Electronics,vol. 27, no. 6, pp. 2813-2824, 2012.

[21] H. Xu, W. Q. Zhang, H. Nian, and J. Li, "Improved vector control of DFIG based wind turbine during grid dips and swells," InIEEEInternational Conference onElectrical Machines and Systems (ICEMS), 2010, pp. 511-515.

[22] J. Hu, H. Nian, H. Xu, and Y. He, "Dynamic modeling and improved control of DFIG under distorted grid voltage conditions,"IEEE Transactions on Energy Conversion,vol. 26, no. 1, pp. 163-175, 2011.

[23] H. Nian, Y. Song, P. Zhou, and Y. He, "Improved direct power control of a wind turbine driven doubly fed induction generator during transient grid voltage unbalance,"IEEE Transactions on Energy Conversion,vol. 26, no.3, pp. 976-986, 2011.

[24] Z. Xie, X. Zhang, X. Zhang, S. Yang, and L. Wang, "Improved ride-through control of DFIG during grid voltage swell,"IEEE Transactions on Industrial Electronics,vol. 62, no. 6, pp. 3584-3594, 2015.

[25] J. Rodriguez, M.P. Kazmierkowski, J.R. Espinoza, P. Zanchetta, H. A. Rub, H.A. Young, and C.A. Rojas, "State of the art of finite control set model predictive control in power electronics,"IEEE Transactions on Industrial Informatics,vol. 9, no. 2, pp. 1003-1016, 2013.

[26] E. Tremblay, S. Atayde, and A. Chandra, "Comparative study of control strategies for the doubly fed induction generator in wind energy conversion systems: a DSP-based implementation approach,"IEEE Transactions on Sustainable Energy,vol. 2, no. 3, pp. 288-299, 2011.

[27] M.K. Döşoğlu, "A new approach for low voltage ride through capability in DFIG based wind farm," International Journal of Electrical Power and Energy Systems,vol. 83, pp. 251-258, 2016.

[28] Manaullah, A.K. Sharma, H. Ahuja, and A. Singh, "Performance comparison of DFIG and SCIG based wind energy conversion systems," In Innovative Applications ofComputational Intelligence on Power, Energy and Controls with their impact on Humanity, pp. 285-290, November 2014.

[29] S.K.Tiwari, B. Singh, and P.K. Goel, "Design and control of microgrid fed by renewable energy generating sources,"IEEE Transactions on Industry Applications,vol. 54, no. 3, pp. 2041-2050, 2018.

[30] D.S. L. Simonetti, A.E. A. Amorim, and F.D. C. Oliveira, "Doubly fed induction generator in wind energy conversion systems," InAdvances in Renewable Energies and Power Technologies, pp. 461-490, 2018.

[31] Y. Deng, Z. Xing, and Q. Zhang, "Analysis of electromagnetic transient characteristics of doubly-fed induction generator under grid voltage swell,"CPSS Transactions on Power Electronics and Applications,vol. 3, no. 2, pp. 111-118, 2018.

[32] S. E. D. Silveira, S. M. Silva, and B. J. C. Filho, "Fault ride-through enhancement in DFIG with control of stator flux using minimized series voltage compensator,"IET Renewable Power Generation,pp.1234-1240, April 2018.

[33] A. Panda and M. Tripathy, "Optimal power flow solution of wind integrated power system using modified bacteria foraging algorithm,"International Journal of Electrical Power and Energy Systems,vol. 54, pp. 306-314, 2014.

[34] E.B. Muhando, T. Senjyu, A. Uehara, and T. Funabashi, "Gain-Scheduled H ∞ Control for WECS via LMI Techniques and Parametrically Dependent Feedback Part II: controller design and implementation,"IEEE Transactions on Industrial Electronics,vol. 58, no. 1, pp. 57-65, 2011.

[35] M. Yamamoto and O. Motoyoshi, "Active and reactive power control for doubly-fed wound rotor induction generator," IEEE Transaction on Power Electronics, vol. 6, no. 4, pp. 624-629, 1991.